Bandpass Filtering of DNA Elastic Modes Using Confinement and Tension

Lin, Jun; Persson, Fredrik; Fritzsche, Joachim; Tegenfeldt, Jonas; Saleh, Omar A.

Published in:
Biophysical Journal

DOI:
10.1016/j.bpj.2011.11.4014

2012

Bandpass Filtering of DNA Elastic Modes Using Confinement and Tension

Jun Lin,[†] Fredrik Persson,[‡] Joachim Fritzsche,[‡] Jonas O. Tegenfeldt,[‡] and Omar A. Saleh[†§*]
[†]Biomolecular Science and Engineering Program, University of California, Santa Barbara, California; [‡]Physics Department, University of Gothenburg, Gothenburg, Sweden; and [§]Materials Department, University of California, Santa Barbara, California

ABSTRACT During a variety of biological and technological processes, biopolymers are simultaneously subject to both confinement and external forces. Although significant efforts have gone into understanding the physics of polymers that are only confined, or only under tension, little work has been done to explore the effects of the interplay of force and confinement. Here, we study the combined effects of stretching and confinement on a polymer's configurational freedom. We measure the elastic response of long double-stranded DNA molecules that are partially confined to thin, nanofabricated slits. We account for the data through a model in which the DNA's short-wavelength transverse elastic modes are cut off by applied force and the DNA's bending stiffness, whereas long-wavelength modes are cut off by confinement. Thus, we show that confinement and stretching combine to permit tunable bandpass filtering of the elastic modes of long polymers.

INTRODUCTION AND BACKGROUND

Long polymers are highly dynamic structures that, when free in solution, adopt self-avoiding random-walk configurations. Such a stochastic structure is not well suited to polymer transport or analysis, nor to external access to heteropolymer sequence. Polymers are thus frequently extended by imposing an external constraint, such as applied tension or confinement. Although the effects of an individual constraint are relatively well understood (1–7), the effects of combining constraints have only been investigated in certain situations (8,9), and so are not as well developed. Yet, in many practical situations, long biological polymers and filaments are subject to both force and confinement. For example, cytoskeletal filaments are confined by the gel-like cytoplasm while subject to external compressive loads (10); nascent proteins are confined by the ribosomal exit pore and stretched by folding of the already extruded domains (11); and certain phage DNAs are confined by a tight portal while being pulled into the infected cell (12,13). Similar confinement/force geometries are achieved in devices that analyze biopolymer length or sequence through application of electric, hydrodynamic or steric forces to polymers confined within gels, nanofabricated channels (3,14,15), or electrically sensed pores (16,17).

Both force and confinement act to constrain the states available to statistical (Kuhn) segments of a polymer, altering its global configuration. This can be analyzed by comparing the length of a Kuhn segment, l, to the characteristic length scale of the constraint. For confinement within a hard-wall pore or slit, the characteristic length is D, the pore diameter or distance between walls; for a polymer under applied tension F, the appropriate scale is the tensile screening length, $\xi = k_B T/F$, where T is the temperature and k_B is Boltzmann's constant. The polymer is only loosely constrained if D or ξ is large relative to l (but smaller than the polymer's radius of gyration); in this limit, the polymer still locally forms a random walk, and the configuration is well described by blob models (2,6). In the tightly constrained regime, where D or ξ is small relative to l, the polymer approaches a perfectly straight configuration and can be modeled by analyzing the remaining slight thermal fluctuations (1,5). Experiments support the models in both regimes of applied tension (4,7), and at least partially support the models of confinement (14,15,18,19).

In nearly all the applications cited above, the polymer is highly stretched. Thus, in our analysis of combining two constraints, we focus on that regime. In particular, we consider a polymer that is tightly constrained by force, $\xi < l$, and develop a model for the effects of confining such a highly stretched polymer. Our model has the expected behavior in the limits when the tension or the confinement dominates, and we present experimental data that verify the model in both limits.

MODEL

We consider a semiflexible polymer, with persistence length A and contour length L, in a long, wide slit of depth D, and stretched with a force F (Fig. 1). When stretched but unconfined, the lateral excursions of a long segment of contour length s will grow in one dimension as a random walk of tensile screening lengths: $\langle R^2_{\perp,1D}(s)\rangle = s\xi$ (5). When confined, these lateral excursions will carry the polymer into contact with the confining walls. Polymer/wall contact will occur within a characteristic contour length s_c defined by $\sqrt{\langle R^2_{\perp,1D}(s_c)\rangle} \approx D/2$, giving $s_c \approx D^2/(4\xi)$.

In analogy to the Odijk picture of a confined polymer (1), we posit that the confined, stretched polymer will act as a chain of independent segments, each of length s_c. This implies that long chains ($L >> s_c$) cannot support modes with wavelengths $>s_c$, or, equivalently, that modes with wavenumber $q < q_c = 8\pi\xi/D^2$ are attenuated (a similar conclusion was made in a recent study of filament buckling within the cytoplasm, in which the confining gel-like cytoskeleton was found to cut off long-wavelength microtubule bending modes (10)). We implement this constraint by

Submitted September 7, 2011, and accepted for publication November 23, 2011.

*Correspondence: saleh@engr.ucsb.edu or saleh@engineering.ucsb.edu

Editor: Laura Finzi.

0006-3495/12/01/0096/5 $2.00

doi: 10.1016/j.bpj.2011.11.4014

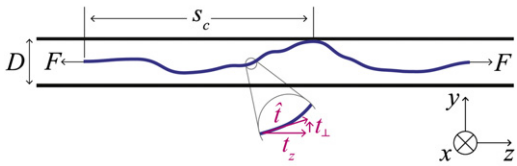

FIGURE 1 Schematic of a doubly constrained polymer. A long semiflexible polymer is stretched with a force F in the z direction, confined in y by a slit of depth D, and unconfined in x. Thermal fluctuations carry the polymer into the wall over a characteristic length s_c.

decomposing the polymer configuration into normal modes: for large forces ($F > k_BT/A \approx 0.1$ pN for DNA) in the $\hat{z}$ direction, lateral fluctuations are small, $t_z >> t_\perp$, where $\hat{t}(s)$ is the unit tangent vector, and the normal modes are described by the amplitudes of lateral sinusoidal waves of wavenumber q. Application of thermal equilibrium for each mode returns the net lateral fluctuations of the chain as the integral over the spectral power (5). In one lateral dimension, this gives

$$\left\langle t^2_{\perp,1D} \right\rangle = 2\int_{q_c}^{\infty} \frac{dq}{2\pi} \frac{\xi}{\xi A q^2 + 1}. \quad (1)$$

That confinement and stretching combine to bandpass-filter polymer elastic modes is clear in Eq. 1: the Lorentzian form of the integrand acts to cut off lateral fluctuations with wavenumbers greater than $q_f = 1/\sqrt{\xi A}$, whereas the lower limit of the integral cuts off fluctuations with wavenumbers less than $q_c = 8\pi\xi/D^2$. Thus, stretching creates a low-pass filter with a cutoff of q_f, and confinement creates a high-pass filter with cutoff q_c, as illustrated in Fig. 2.

The total lateral fluctuations, $\langle t^2{}_\perp \rangle = \langle t^2{}_x \rangle + \langle t^2{}_y \rangle$, are related to the relative extension, z/L, through $z/L = 1 - \langle t^2{}_\perp \rangle/2$ (5). If the polymer is equally confined in two dimensions, both lateral dimensions can be found from Eq. 1. Here, we focus on slit geometries in which the polymer is only confined in y. The fluctuations in the confined direction, $\langle t^2{}_y \rangle$, are given by Eq. 1, whereas those in the unconfined direction, $\langle t^2{}_x \rangle$, follow from Eq. 1 using $q_c = 0$. The bandpass model then predicts the force-dependent relative extension, $z(F)/L \equiv g_{BP}(F)$, as

$$g_{BP}(F) = 1 - \frac{1}{2}\sqrt{\frac{k_BT}{FA}}\left[1 - \frac{1}{\pi}\tan^{-1}\left(\frac{8\pi}{D^2}\sqrt{A\left(\frac{k_BT}{F}\right)^3}\right)\right]. \quad (2)$$

Our derivation is based on a scaling picture, and so does not directly account for microscopic details of the system. Thus, although our model dictates that modes are attenuated below q_c, the shape of the attenuation is not known. Equation 2 assumes a sharp cutoff at q_c. An alternate analytical expression can be derived using a more gentle roll-off (see Fig. S1 and Section SA in the Supporting Material); however, this expression gives near-identical results to Eq. 2, and we use Eq. 2 in all analysis that follows.

We expect confinement to negligibly affect elasticity if either the slit depth is large or the force is high; in these limits, the polymer never interacts with the slit, and fluctuations are equally constrained by the force in both lateral dimensions. Accordingly, for large D or F, g_{BP} asymptotically approaches the Marko-Siggia (MS) expression for the high-force relative extension (5),

$$g_{MS,2D}(F) = 1 - \frac{1}{2}\sqrt{k_BT/FA}.$$

Conversely, if D or F are small, confinement will constrain the polymer in one lateral dimension, and force in the other. In this limit, the polymer's elastic response is dictated by only the unconfined dimension, as the fluctuations in the confined dimension do not vary with force. Accordingly, for small D or F, g_{BP} asymptotically approaches the Marko-Siggia expression for a polymer with only one lateral degree of freedom,

$$g_{MS,1D}(F) = 1 - \frac{1}{4}\sqrt{k_BT/FA}.$$

In sum, the bandpass model interpolates between situations where the polymer has one or two degrees of lateral freedom, as can be seen in Fig. 2. The model quantifies the deformation of a polymer that is both highly stretched and subject to confinement in a slit; the asymptotic behavior of Eq. 2 indicates that the model holds for all regimes of confinement.

In many cases, only part of the polymer is confined. Generally, this can be accounted for by applying the constraints that the tension is constant throughout the polymer, and that the total polymer length is constant. To

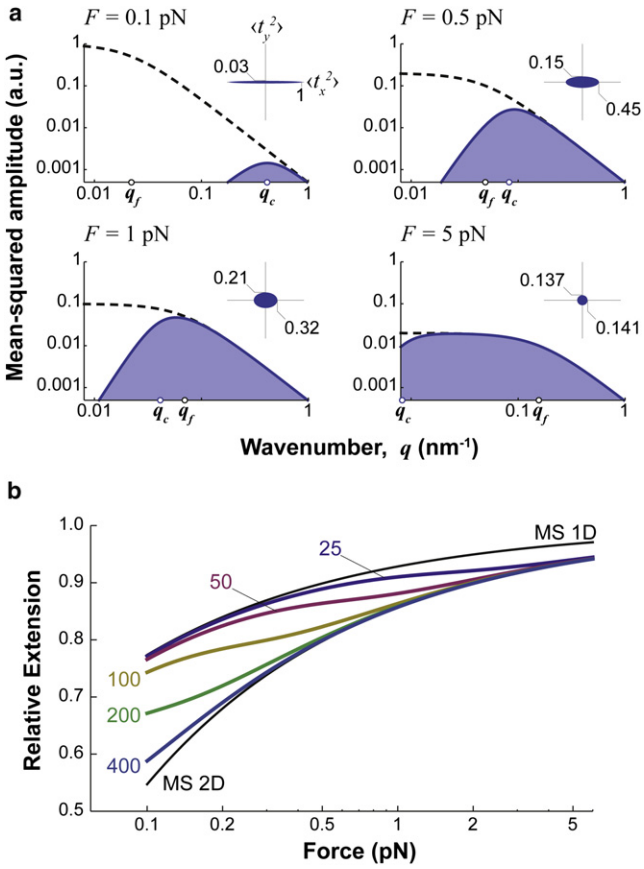

FIGURE 2 Principle and predictions of the bandpass model. (*a*) Power-spectra of fluctuations of $t_\perp$, the lateral component of the unit tangent vector, calculated for a DNA molecule in a 50-nm-deep slit over a range of forces. Values are normalized to the maximum mean-squared amplitude at lowest force. Stretching alone (*dashed line*) attenuates modes with $q > q_f$; the area under this curve gives the net lateral fluctuation, $\langle t^2{}_x \rangle$, in the unconfined direction. The addition of confinement (*solid line*) attenuates modes below q_c; the area under this line gives the net fluctuations, $\langle t^2{}_y \rangle$, in the confined direction. (*Inset*) Net lateral fluctuations, with values normalized to $\langle t^2{}_x \rangle$ at 0.1 pN. Fluctuations in y are frozen out at low forces, giving $\langle t^2{}_x \rangle >> \langle t^2{}_y \rangle$, whereas higher forces broaden the pass-band, resulting in symmetric fluctuations. (*b*) Bandpass-model predictions for the force-extension behavior of a DNA molecule confined to slits of a variety of depths (as labeled, in nm). Also plotted are the Marko-Siggia (unconfined) predictions (5), assuming fluctuations are allowed in one (MS 1D) or two (MS 2D) lateral dimensions.

compare to our experiment on confined DNA (Fig. 3), we also require that the DNA always extends across the slit of length z_s, and always extends the distance z_T from the slit to the tether point. Using $g_{BP}(F)$ for the confined portion of the polymer and $g_{MS,2D}(F)$ for the unconfined portion, we predict the distance between the slit edge and the bead, z_B, to vary with force as

$$z_B(F) = Lg_{MS,2D}(F) - \frac{g_{MS,2D}(F)}{g_{BP}(F)}z_s - z_T. \quad (3)$$

This is the force-extension prediction to which we compare our data; note that, because D, A, and z_s are known, the only free parameter is the tether-side extension z_T.

MATERIALS AND METHODS

Microfluidic devices are constructed by etching slits and reservoirs into fused silica, and sealing by thermal fusion bonding to a fused silica coverslip (see Section SC3 in the Supporting Material). One reservoir (the tether-side reservoir, Fig. 3) is functionalized by flowing in an antibody to digoxigenin, and allowing it to adhere to the reservoir walls. Then, the other reservoir is infused with 1-μm-diameter magnetic beads bound through biotin/streptavidin linkages to λ-phage DNA. By inducing a cross-flow through the slits, a small number of DNA molecules are made to thread the slits; the molecules could not fully pass through due to the large size of the attached magnetic bead. The digoxigenin-labeled DNA terminus of some of these molecules then bound itself to the antibody in the functionalized reservoir.

After shutting off the fluid flow, DNA is stretched by bringing a pair of small magnets in proximity to the chip, attracting the magnetic bead. We use optical bead tracking to measure the bead's position, and thus the DNA extension, with respect to the slit edge (see Section SC1 in the Supporting Material). The bead is pulled both laterally and vertically by the applied field; full three-dimensional bead tracking is achieved by prior calibration of the magnitude and pulling angle of the force (see Section SC2 in the Supporting Material). Each measurement of extension (i.e., each point in the force/extension curve) is based on several minutes of bead-tracking at constant force, and with a 60-Hz frame rate. We estimate errors in the extension from the quadrature sum of 1), the error in determining the bead center from the image (a constant 50-nm error for each point), and 2), the uncertainty derived from the spread in calibration-curve angles. The error in force is estimated from the spread in calibration-curve forces. We discard data points in which the bead approaches either the slit edge, or the top of the 6-μm tall reservoir, as the bead/wall interactions obscure the DNA elastic response. Finally, we discard any data showing significant bead motion in a direction normal to the magnetic force (i.e., motion caused by remnant fluid flow in the reservoir).

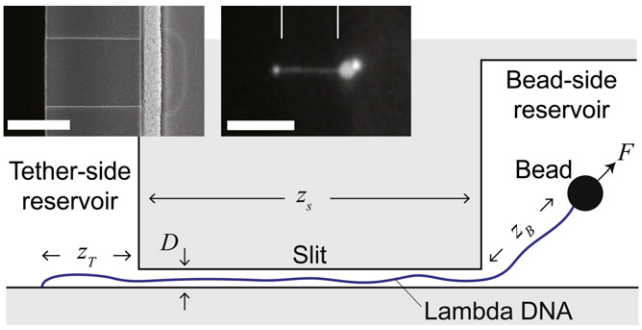

FIGURE 3 Experimental geometry. A DNA molecule is threaded through a slit between two reservoirs on a microfabricated chip. It is tethered to the surface of one reservoir, and to a magnetic bead in the other. An external magnetic field manipulates the bead, applying a known stretching force to the DNA; optical bead tracking gives a direct measure of the extension z_B of the DNA in the bead-side reservoir. (*Insets*) An electron micrograph of a slit (*left*) and an optical image of a fluorescently stained DNA threading a slit (*right*). The autofluorescent bead is clearly visible. (*Overlaid open lines*) The extent of the slit. Scale bars, 5 μm.

RESULTS

We measure the force-extension behavior of λ-phage DNA molecules ($L = 16.5$ μm) that connect two large reservoirs by threading through a nanofabricated slit (Fig. 3). We use slits of depths $D = 50$, 90, and 160 nm, and lengths $Z_s = 5.7$–9.3 μm; all slits are 5-μm wide. The DNA is stretched by immobilizing both ends, one to the reservoir surface and the other to a magnetic bead, and applying a magnetic field. We calibrate the stretching force using standard methods of single-molecule manipulation (see Fig. S3); accessible forces are between 0.1 and 2 pN, and forces are known to be better than 10%. The device geometry forces the DNA to be pulled against the slit wall at one edge, which will likely increase the effect of confinement at that edge. However, we expect this effect to be negligible, as the localization of the DNA to the wall will decay within roughly a persistence length, which is much less than the total length of the slit.

The force-extension data are in excellent agreement with the bandpass model, as can be seen in Fig. 4. In that figure, Eq. 3 is fit to the data with only z_T as a free parameter, and with $k_BT = 4.1$ pN nm, as appropriate for room temperature, and $A = 50$ nm, as appropriate for DNA. The best-fit z_T values tend to vary inversely with slit depths. This is reasonable, as larger hydrostatic pressures are needed to push the DNA into the smaller slits for initial tethering; the resulting high fluid flow speeds push the tether point farther from the slit.

We can also compare the measured elasticity to that predicted by the Marko-Siggia model for a polymer allowed to have one or two dimensions of lateral fluctuations. To do this, we use Eq. 3 with the z_T value estimated from the bandpass-model fit, and then substitute either $g_{MS,2D}$ or $g_{MS,1D}$ for g_{BP}; the results are plotted in Fig. 4. As expected, the data interpolate between a regime where force affects only one lateral dimension of the DNA (with the other dimension frozen by confinement), and a regime where force affects both lateral dimensions. Finally, we can test the robustness of the model fitting by comparing predictions using the best-fit z_T, but varying slit depths (see Fig. S2 and Section SB in the Supporting Material); we find that variations of D indeed systematically deviate from the data, indicating that the model is sensitive to q_c.

DISCUSSION

In conclusion, we have presented a theoretical and experimental treatment of the elasticity of confined polymers.

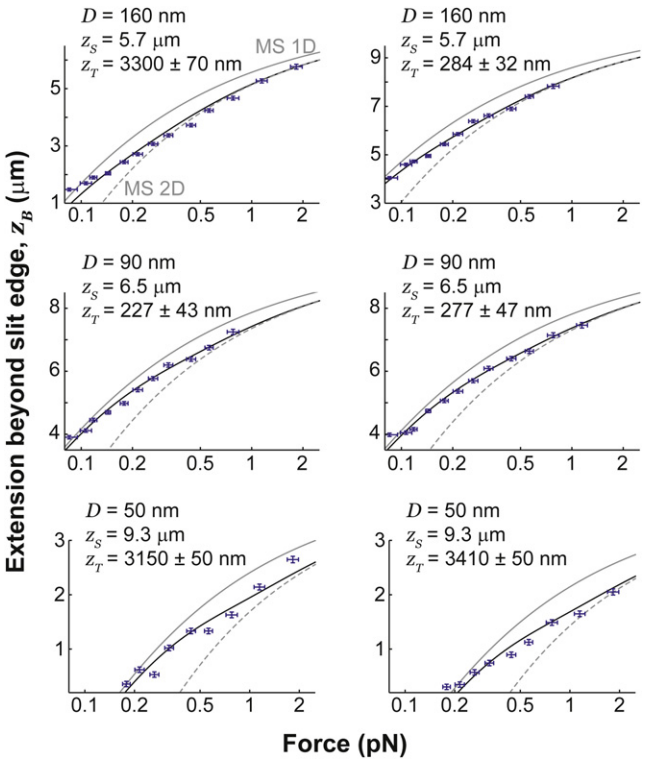

FIGURE 4 Comparison of stretching data to the bandpass model. Force-extension data (*points*) for λ-DNA partially confined to slits of depth D and length z_S, as indicated, were fit by the bandpass model predictions (*solid line*; Eqs. 2 and 3) using only the tether-side extension, z_T, as a free parameter. Best-fit values of z_T are indicated. The same values of z_T were used to plot the Marko-Siggia prediction for polymers with lateral fluctuations in either one (*shaded line*) or both (*dashed line*) dimensions.

Our theory starts with the Marko-Siggia picture of the thermally actuated elastic fluctuations of a stretched polymer, and adjusts it by adding a length scale describing collisions of the polymer with walls. This corresponds to imposing a long-wavelength cutoff of the polymer's elastic modes; thus, in combination with the short-wavelength cutoff imposed by the force and the polymer's intrinsic bending rigidity, we predict that confinement and stretching combine to bandpass-filter the elastic modes of a polymer. We tested this theory by measuring the elasticity of long DNA molecules partially confined in slits of varying geometry, and found that the bandpass theory quantitatively describes the experimental data.

The ability to controllably allow thermal excitation of certain elastic modes of a biopolymer is intriguing, as it is known that functionally important motions of catalytically active proteins frequently correspond to the protein's normal modes (20,21). We speculate that theory and methods analogous to those developed here can be adapted to implement control of the elastic modes of enzymes, and thus control of enzymatic activity. Of course, we cannot rule out the possibility that biology has already discovered and implemented such a mechanism.

SUPPORTING MATERIAL

Additional sections with supporting equations, supporting methods, four figures, and references (22–24) are available at http://www.biophysj.org/biophysj/supplemental/S0006-3495(11)05366-5.

This work was supported by a Young Investigators' Grant from the Human Frontier Science Program (RGY0078/2007-C), Swedish Research Council grants 2007-584 and 2007-4454, and the National Science Foundation under grant DMR-1006737.

REFERENCES

1. Odijk, T. 1983. On the statistics and dynamics of confined or entangled stiff polymers. *Macromolecules.* 16:1340–1344.
2. de Gennes, P. G. 1979. Scaling Concepts in Polymer Physics. Cornell University Press, Ithaca, NY.
3. Persson, F., and J. O. Tegenfeldt. 2010. DNA in nanochannels—directly visualizing genomic information. *Chem. Soc. Rev.* 39:985–999.
4. Bustamante, C., J. F. Marko, …, S. Smith. 1994. Entropic elasticity of λ-phage DNA. *Science.* 265:1599–1600.
5. Marko, J. F., and E. D. Siggia. 1995. Stretching DNA. *Macromolecules.* 28:8759–8770.
6. Pincus, P. 1976. Excluded volume effects and stretched polymer chains. *Macromolecules.* 9:386–388.
7. Saleh, O. A., D. B. McIntosh, …, N. Ribeck. 2009. Nonlinear low-force elasticity of single-stranded DNA molecules. *Phys. Rev. Lett.* 102:068301.
8. Luo, K., and R. Metzler. 2011. The chain sucker: translocation dynamics of a polymer chain into a long narrow channel driven by longitudinal flow. *J. Chem. Phys.* 134:135102.
9. Sakaue, T. 2010. Sucking genes into pores: insight into driven translocation. *Phys. Rev. E.* 81:041808.
10. Brangwynne, C. P., F. C. MacKintosh, …, D. A. Weitz. 2006. Microtubules can bear enhanced compressive loads in living cells because of lateral reinforcement. *J. Cell Biol.* 173:733–741.
11. Cabrita, L. D., C. M. Dobson, and J. Christodoulou. 2010. Protein folding on the ribosome. *Curr. Opin. Struct. Biol.* 20:33–45.
12. Löf, D., K. Schillén, …, A. Evilevitch. 2007. Forces controlling the rate of DNA ejection from phage lambda. *J. Mol. Biol.* 368:55–65.
13. Inamdar, M. M., W. M. Gelbart, and R. Phillips. 2006. Dynamics of DNA ejection from bacteriophage. *Biophys. J.* 91:411–420.
14. Reisner, W., K. J. Morton, …, R. H. Austin. 2005. Statics and dynamics of single DNA molecules confined in nanochannels. *Phys. Rev. Lett.* 94:196101.
15. Persson, F., P. Utko, …, A. Kristensen. 2009. Confinement spectroscopy: probing single DNA molecules with tapered nanochannels. *Nano Lett.* 9:1382–1385.
16. Zwolak, M., and M. Di Ventra. 2008. Colloquium: physical approaches to DNA sequencing and detection. *Rev. Mod. Phys.* 80:141–165.
17. Keyser, U. F., B. N. Koeleman, …, C. Dekker. 2006. Direct force measurements on DNA in a solid-state nanopore. *Nat. Phys.* 2:473–477.
18. Jo, K., D. M. Dhingra, …, D. C. Schwartz. 2007. A single-molecule bar-coding system using nanoslits for DNA analysis. *Proc. Natl. Acad. Sci. USA.* 104:2673–2678.
19. Kim, Y., K. S. Kim, …, D. C. Schwartz. 2011. Nanochannel confinement: DNA stretch approaching full contour length. *Lab Chip.* 11:1721–1729.
20. Bahar, I., C. Chennubhotla, and D. Tobi. 2007. Intrinsic dynamics of enzymes in the unbound state and relation to allosteric regulation. *Curr. Opin. Struct. Biol.* 17:633–640.

21. Zhuravlev, P. I., and G. A. Papoian. 2010. Protein functional landscapes, dynamics, allostery: a tortuous path towards a universal theoretical framework. *Q. Rev. Biophys.* 43:295–332.

22. Ribeck, N., and O. A. Saleh. 2008. Multiplexed single-molecule measurements with magnetic tweezers. *Rev. Sci. Instrum.* 79:094301.

23. Gosse, C., and V. Croquette. 2002. Magnetic tweezers: micromanipulation and force measurement at the molecular level. *Biophys. J.* 82:3314–3329.

24. Strick, T. R., J. F. Allemand, …, V. Croquette. 1996. The elasticity of a single supercoiled DNA molecule. *Science.* 271:1835–1837.